ISSN 0020-4412, Instruments and Experimental Techniques, 2020, Vol. 63, No. 5, pp. 616–620. © Pleiades Publishing, Ltd., 2020.

NUCLEAR EXPERIMENTAL TECHNIQUE

Development of a Compact Deuterium–Deuterium Neutron Generator for Prompt Gamma Neutron Activation Analysis

Ke Jian-Lin[a],*, Liu Yu-Guo[a], Liu Bai-Li[a], Hu Yong-Hong[a], Liu Meng[a], Tang Jun[a], Zheng Pu[a], Li Yan[a], Wu Chun-Lei[a], and Lou Ben-Chao[a]

[a] *Institute of Nuclear Physics and Chemistry, CAEP, Mianyang, 621000 China*

**e-mail: kejl1@qq.com*

Received February 16, 2020; revised March 17, 2020; accepted March 18, 2020

Abstract—A compact deuterium–deuterium neutron generator for prompt gamma neutron activation analysis was developed at Institute of Nuclear Physics and Chemistry. A neutron yield of 3.6×10^8 s^{-1} was achieved during of the bombardment of a titanium drive-in target by a 6.8 mA deuteron beam at 115 keV. The deuteron beam was generated by a permanent magnet microwave ion source. An 85 h long run with 1.2×10^8 s^{-1} average neutron yield was performed at 85 keV and 3.7 mA. The operating mode of the neutron generator reached 99.95%.

DOI: 10.1134/S0020441220050036

1. INTRODUCTION

Neutron generators are widely used in neutron science [1], material analysis [2], explosive detection [3], neutron radiography [4] and so on. A compact deuterium–deuterium neutron generator has been developed at Institute of Nuclear Physics and Chemistry for an on-line coal quality analyzer, which is used to detect the bulk elements of coals by prompt gamma neutron activation analysis. Compared with radio-isotopic neutron generator and deuterium–tritium (D–T) neutron generator, deuterium–deuterium (D–D) neutron generator has many advantages. Firstly, D–D neutron generator is safer. It is nearly free from tritium contamination and can be turned off in the case of installation and transportation. Secondly, the deuterium in the target can be complemented by the incident deuterium ions, thus the lifetime of the D–D neutron generator is generally very long. Thirdly, the D–D neutron generator does not require complex maintenance, as its components are replaceable and stops emitting when turned off.

Various efforts have been made to develop compact D–D neutron generators all over the world [5–10]. In this work, a compact D–D neutron generator using a titanium drive-in target was designed and tested with a designed yield of 3×10^8 s^{-1}.

2. NEUTRON GENERATOR DESIGN

A schematic structure of the neutron generator is shown in Fig. 1. It was mainly composed of a permanent magnet microwave ion source and a titanium drive-in target. The ion source and the vacuum chamber of the generator were at the ground potential. The titanium drive-in target, wrapped in the outer shell, was at the negative high potential. Thus, there was no high voltage where people can reach. The differential cross section of the deuterium-deuterium reaction at 0° is about two times of that at 90° [11]. To avoid the neutrons at zero degree are intercepted, the water and the bias voltage were supplied to the target at a 90° angle.

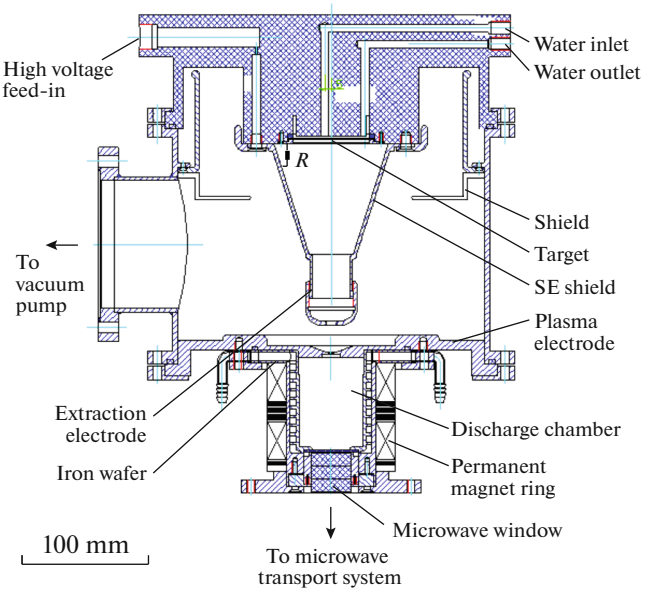

Fig. 1. Schematic drawing of the D–D neutron generator.

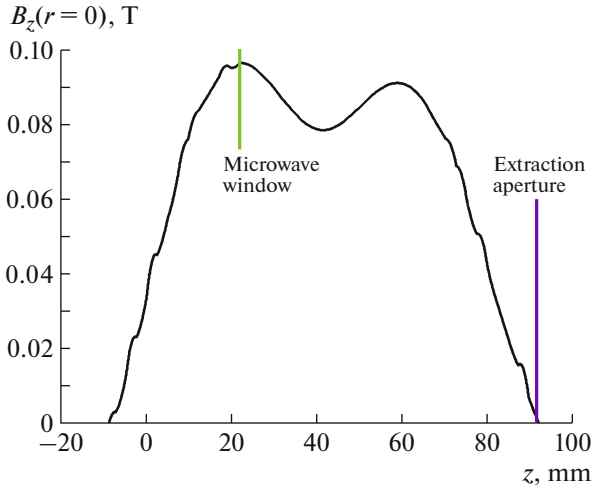

Fig. 2. The axial magnetic field along the source axis.

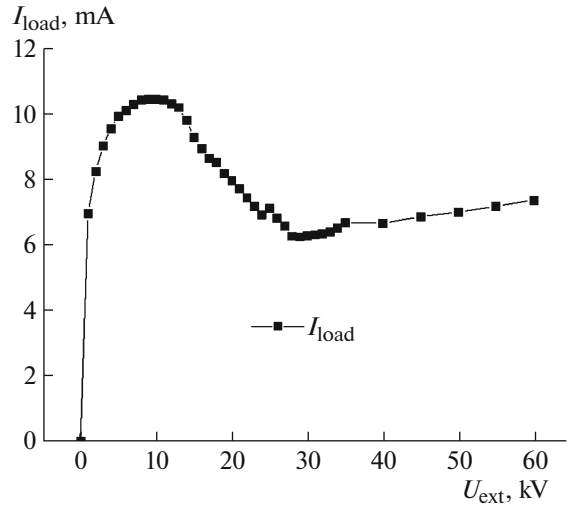

Fig. 3. Variation of the load current I_{load} of the high-voltage power supply with the extraction voltage U_{ext}.

As shown in Fig. 1, a permanent magnet microwave ion source was used in the compact D-D neutron generator for its long lifetime, high stability and relatively intense ion beam. The discharge chamber of the microwave ion source was 50 mm in diameter and 70 mm in length. The discharge chamber was made of stainless steel. The microwave power was generated by a 2.45 GHz/1.5 kW magnetron and transported to the discharge chamber through an isolator, a three-stub tuner, a 90° microwave bend and a dielectric window. The dielectric window was composed of a ∅31 × 30 mm aluminum column and a 2 mm thick BN disk.

The magnetic field for plasma producing was formed by two NdFeB magnet rings with B_r =1.3 T. The dimensions of the rings were inner diameter of 70 mm and outer diameter of 95 mm and thickness of 30 mm. The gap between two rings was 14 mm to form a saddle-like axial magnetic field profile, as suggested by Peng et al. [12] and Liu et al. [13]. An iron wafer with thickness of 1mm was used to shield the magnetic field and to decrease the probability of discharge between the extraction electrode and the discharge chamber. The measured axial magnetic field along the source axis is shown in Fig. 2.

The deuterons were extracted by a three-electrodes system, which was composed of a plasma electrode, an extraction electrode and a target. The diameters of the apertures on the plasma electrode and the extraction electrode were 4 and 8 mm, respectively. The distance between the two apertures was adjustable within the 15–30 mm range. The diameter of the target was 60 mm. The designed potentials of the plasma electrode and the extraction electrode was 0 V and −120 kV, respectively.

The SE shield electrode, which was electrically connected with the extraction electrode, was used to shield the secondary electrons generated from the target. The SE shield and the target were electrically connected by a resistance with the value of 50 kΩ. Thus, the potential difference between the target and the SE shield reached hundreds of volts while the negative high voltage supplied to the SE shield. This potential difference would prohibit the secondary electrons and push them back to the target. The probability of breakdown between the plasma electrode and the extraction electrode decreased. The deuteron beam current of the D–D neutron generator could be estimated by the load current of the high-voltage power supply, as long as the deuterons were not bombarding on the extraction electrode. Figure 3 shows the variation of the load current of the high-voltage power supply with the deuteron energy. The load current of the high-voltage power supply, I_{load}, can be expressed as:

$$I_{load} = I_{d,target} + I_{d,ext}(1 + \gamma) = I_{d,tot} + I_{d,ext}\gamma, \quad (1)$$

where $I_{d,\,target}$ is the deuteron current on the target, and $I_{d,\,ext}$ is the deuteron current on the extraction elec-

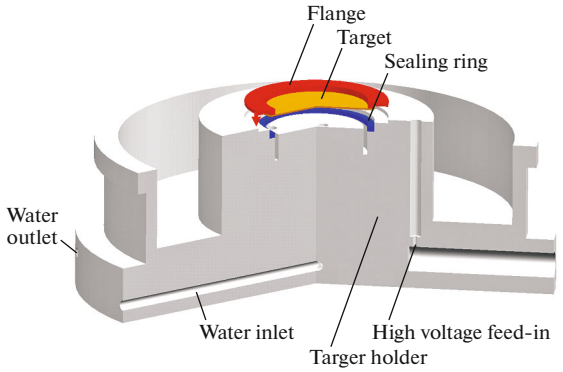

Fig. 4. Drawing of the titanium driven-in target and its assembly.

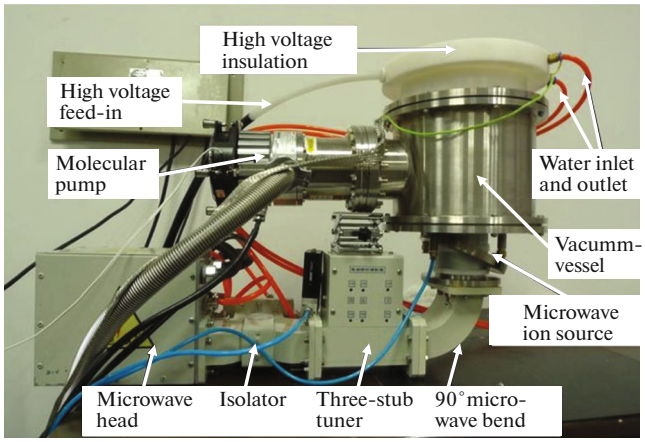

Fig. 5. Photograph of the D–D neutron generator.

trode, and $I_{d,\,tot}$ is the total deuteron current of the neutron generator, and γ is the secondary electron yield. It should be pointed out that the secondary electron yield increased with the increase of deuteron energy in this energy range [14]. In the meanwhile, the plasma sheath edge moved toward to the plasma when the extraction voltage increased [15], thus the beam diverged and then $I_{d,\,ext}$ decreased with the increase of extraction voltage. In Fig. 3, the peak of I_{load} at about 10 keV is the result of the increased secondary electron yield and the decreased $I_{d,\,ext}$. In addition, the slow increase when the voltage more than 28 keV should be attributed to the tiny increase of the emission area, due to the move of the plasma sheath edge.

Figure 4 shows a detailed drawing of the titanium drive-in target and the target assembly. The target was directly cooled by de-ionized water and could be easily replaced after use. Jet impingement cooling was applied, and the jet center was displaced 5 mm from the beam center to cool the target more efficiently. The thermal analysis of the titanium drive-in target was discussed elsewhere [16]. The titanium drive-in target was made of a 0.05 mm thick titanium film plated on a 0.5 mm thick copper plate. The driven-in target was a 0.05 mm thick titanium film plated on a 0.5 mm thick copper plate. This was because titanium had a higher neutron yield and copper had a higher thermal conductivity. The titanium film was plated on copper by filter cathode vacuum arc technique [17]. The SE shield and the titanium driven-in target were assembled on a target holder that made of homopolymer, through which bias voltage and cooling water was supplied to the SE shield and the target. De-ionized water was used to cool and insulate the target. The temperature of the water was controlled by a chiller while it was circulating in a closed loop, and the specific resistivity was achieved by a parallel connected ion-exchange-resin column.

3. EXPERIMENTAL RESULTS

Figure 5 shows the assembled D-D neutron generator. The generator was about 0.6 m in length and 0.5 m in height. It could be placed inside the applied device and connected to the controller and the chiller by wires and pipes.

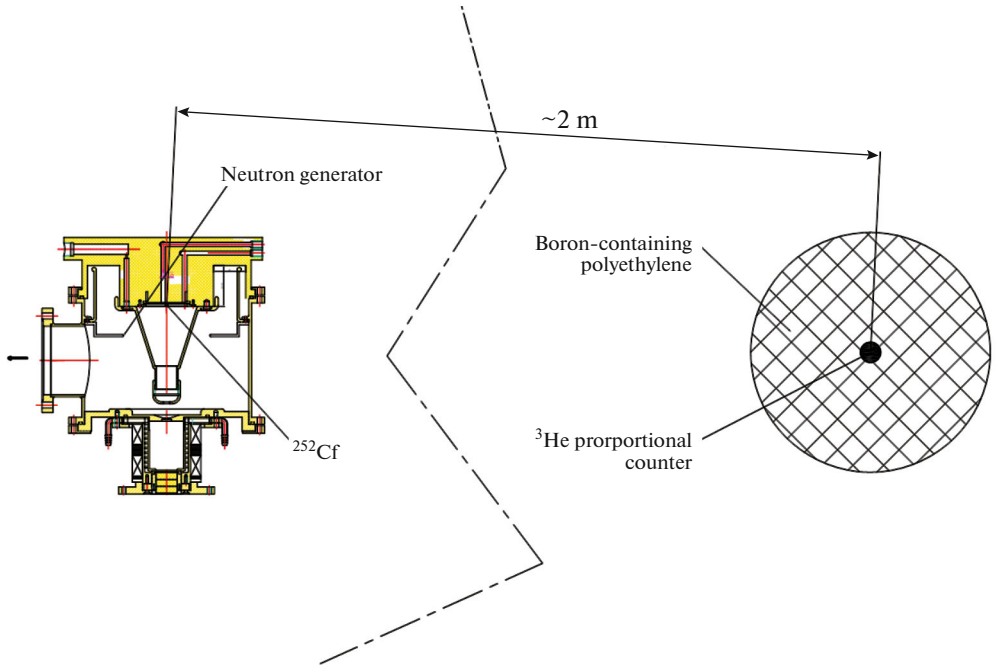

Fig. 6. Layout of the calibration of the ^{3}He proportional counter.

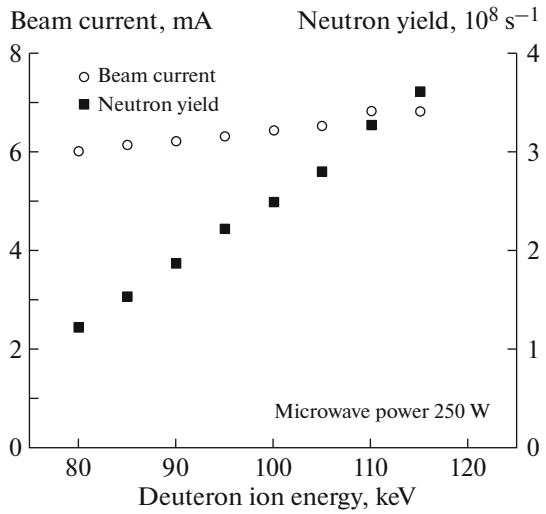

Fig. 7. Variation of beam current and neutron yield with deuterium ion energy at 250 W of microwave power. The hydraulic pressure of the chiller was 2.5 kg/cm^2, and the resistivity of the water had exceeded 16 MΩ cm.

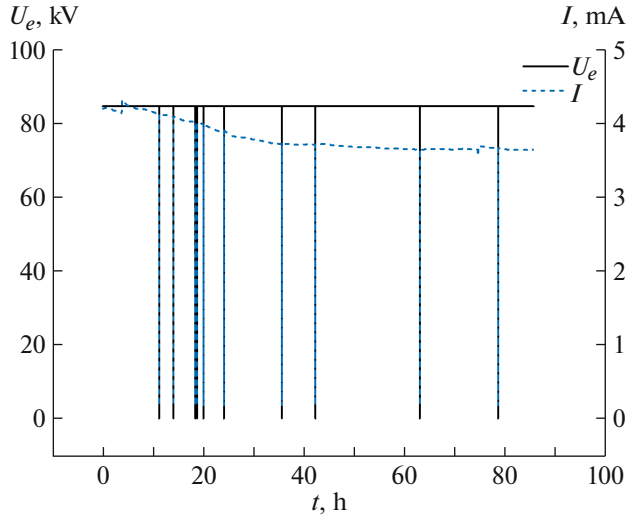

Fig. 8. Extraction voltage and load current in the 85-hours long run. The microwave power was 230 W.

The neutron yield of the D–D neutron generator was measured by a ^{3}He proportional counter. The ^{3}He proportional counter was inserted into a Boron-containing polyethylene tank. The rate of the ^{3}He counter was calibrated by a ^{252}Cf source which was placed to the position of the titanium drive-in target (shown in Fig. 6).

The variation of beam current and neutron yield with deuterium ion energy at 250 W of microwave power is shown in Fig. 7. The hydraulic pressure of the chiller was 2.5 kg/cm^2, and the resistivity of the water had exceeded 16 MΩ cm. The extracted deuteron current and the neutron yield increased with the deuterium ion energy. The neutron yield reached 3.6×10^8 s^{-1} at 115 keV and 6.8 mA.

We performed an 85-h long run when the deuteron energy was 85 keV and mean current was 3.7 mA (Fig. 8). The mean neutron yield was about 1.2×10^8 s^{-1}. The operating mode of the neutron generator reached 99.95%. The sharp drop in neutron yield occurred mainly due to the breakdown of the generator, mostly attributed to the flash-over of the insulator. The restarts of the generator were automatically operated within 20 s.

4. CONCLUSIONS

A compact deuterium-deuterium neutron generator using a permanent magnet microwave ion source and a titanium driven-in target was designed and tested at INPC. A neutron yield of 3.6×10^8 s^{-1} was achieved by bombarding a titanium drive-in target by a 6.8 mA deuteron beam at 115 keV. An 85 h long run with 1.2×10^8 s^{-1} mean neutron yield was performed at 85 keV and 3.7 mA. The operation mode of the neutron generator reached 99.95%.

ACKNOWLEDGMENTS

THANKS to professor Shixiang Peng from Peking University for her help in the design of the microwave ion source. This work was supported by a grant from the National Natural Science Foundation of China (no. 11705174).

REFERENCES

1. Zhu, T.H., Liu, R., Jiang, L., Lu, X.X., Wen, Z.W., Wang, M., and Lin, J.F., *At. Energy Sci. Technol.,* 2008, vol. 42, p. 593. https://doi.org/10.7538/yzk.2008.42.07.0593
2. Vainionpaa, J.H., Chen, A.X., Piestrup, M.A., Gary, C.K., Jones, G., and Pantell, R.H., *Nucl. Instrum. Methods Phys. Res., Sect. B,* 2015, vol. 350, p. 88. https://doi.org/10.1016/j.nimb.2014.12.077
3. Koltick, D., Kim, Y., McConchie, S., Novikov, I., Belbot, M., and Gardner, G., *Nucl. Instrum. Methods Phys. Res., Sect. B,* 2007, vol. 261, p. 277. https://doi.org/10.1016/j.nimb.2007.03.047
4. Fantidis, J.G., Nicolaou, G.E., and Tsagas, N.F., *Nucl. Instrum. Methods Phys. Res., Sect. A,* 2010, vol. 618, p. 331. https://doi.org/10.1016/j.nima.2010.02.107
5. Reijonen, J., Gicquel, F., Hahto, S.K., King, M., Lou, T.-P., and Leung, K.-N., *Appl. Radiat. Isot.,* 2005, vol. 63, p. 757. https://doi.org/10.1016/j.apradiso.2005.05.024
6. Vainionpaa, J.H., Harris, J.L., Piestrup, M.A., Gary, C.K., and Williams, D.L., *AIP Conf. Proc.,* 2013, vol. 1525, p. 118. https://doi.org/10.1063/1.4802303
7. Izotov, I. and Skalyga, V., *AIP Conf. Proc.,* 2016, vol. 1771, p. 090005. https://doi.org/10.1063/1.4964247

8. Huang, Z.-W., Wang, J.-R., Wie, Z., Lu, X.-L., Ma, Z.-W., Ran, J.-L., Zhang, Z.-M., Yao, Z.-E., and Zhang, Y., *J. Instrum.,* 2018, vol. 13, p. P01013. https://doi.org/10.1088/1748-0221/13/01/p01013
9. Adams, R., Bort, L., Zboray, R., and Prasser, H., *Appl. Radiat. Isot.,* 2015, vol. 96, p. 114. https://doi.org/10.1016/j.apradiso.2014.11.017
10. Das, B.K., Shyam, A., Das, R., and Rao, A.D.P., *Instrum. Exp. Tech.,* 2013, vol. 56, no. 2, p. 130. https://doi.org/10.1134/S0020441213010260
11. Drosg, M., DROSG-2000, PC Database for 56 Neutron Source Reactions, IAEA-NDS-87, 2000.
12. Peng, S.X., Xu, R., Zhao, J., Yuan, Z.X., Zhang, M., Song, Z.Z., Yu, J.X., Lu, Y.R., and Guo, Z.Y., *Rev. Sci. Instrum.,* 2008, vol. 79, p. 02A310. https://doi.org/10.1063/1.2812343
13. Liu, Y.G., Ke, J.L., Zhao, G.Y., Lou, B.C., Hu, Y.H., and Liu, R., *Nucl. Sci. Tech.,* 2018, vol. 29, p. 17. https://doi.org/10.1007/s41365-018-0464-3
14. Ke, J.L., Liu, M., and Zhou, C.G., *Nucl. Instrum. Methods Phys. Res., Sect. B,* 2012, vol. 280, p. 1. https://doi.org/10.1016/j.nimb.2012.02.033
15. Brown, I.G., *The Physics and Technology of Ion Source,* Weinheim: Wiley-VCH, 2004.
16. Liu, Y.G., Liu, M., Ke, J.L., Hu, Y.H., Lou, B.C., Jiang, B., Zhao, G.Y., and Liu, R., *Nucl. Tech.,* 2017, vol. 40, p. 010202. https://doi.org/10.11889/j.0253-3219.2017.hjs.40.010202
17. Wu, X.Y., Liao, B., Zhang, X., Li, Q., Peng, J.H., Zhang, H.X., and Zhang, X.J., *J. Beijing Norm. Univ. (Nat. Sci.),* 2014, vol. 50, p. 132. https://doi.org/10.1177/0040517506059708